Angle-resolved and internuclear-separation-resolved measurements of the ionization rate of the B state of I_2 by strong laser fields

H. Chen,[1] L. Fang,[2] V. Tagliamonti,[1] and G. N. Gibson[1]
[1]*Department of Physics, University of Connecticut, Storrs, Connecticut 06269, USA*
[2]*Physics Department, Western Michigan University, Kalamazoo, Michigan 49008, USA*
(Received 12 August 2011; published 24 October 2011)

Angle-resolved and internuclear-separation-resolved measurements of the single ionization rate of neutral I_2 have been obtained. By launching a wave packet in the $B\,^3\Pi_u{}^+$ state (B state) of I_2 with a 50-fs tunable pump pulse we can measure the ionization rate as a function of internuclear separation as the wave packet evolves in the B state. Moreover, since the ground to B-state optical transition dipole moment is parallel to the internuclear axis, the B-state subpopulation of the I_2 thermal ensemble will have a high degree of alignment, allowing for angular measurements. The B state shows the well-known effect of enhanced ionization at a critical separation, R_c, with an enhancement factor of 22 when the ionizing field is polarized along the internuclear axis and the enhanced ionization decreases when the angle between the field and the axis increases from 0° to 90°, finally disappearing at 90°. These results on the enhanced ionization of the B state of I_2 give the most precise determination of R_c for any molecule and agree extremely well with the prediction from a simple model of electron localization.

DOI: 10.1103/PhysRevA.84.043427 PACS number(s): 33.80.Rv, 32.80.Rm, 42.50.Hz

I. INTRODUCTION

In most situations of the interaction of diatomic molecules with intense laser fields, the tunneling ionization rate increases as a function of the internuclear distance R, reaches a significantly high peak at a certain critical internuclear separation, R_c, and then decreases. This very general phenomenon, known as enhanced ionization (EI), is invoked in many experiments [1–3].

EI has been explored in a number of cases both experimentally and theoretically. The simplest example is one electron in a double well, such as $H_2{}^+$. It has been shown that the effects leading to EI in this case are charge-resonance-enhanced ionization (CREI) and electron localization [4,5]. CREI is a combination of the field-induced barrier suppression and the strong coupling between the charge-resonant states. The former allows for fast ionization from the upper state at a certain critical internuclear separation, and the latter guarantees a sufficient population in the upper-level state through nonadiabatic excitation from the lower state [4]. The calculations have been verified by experimental studies of EI in $H_2{}^+$ [1,2]. In addition, EI in $H_2{}^+$ as a function of the angle θ between the molecular axis and the field polarization has been calculated and found to decrease as the angle increases, finally disappearing at 90° [6]. However, this has not yet been demonstrated experimentally.

EI can also occur in more complex systems. In the one-electron case, it is shown theoretically that EI is highly dependent on the molecular symmetry and only occurs for σ states, not for π or δ states [7]. In the case of two-electron equivalent states in neutral H_2, it is believed that EI is due to the ionic states working as doorway states [8,9]. One experiment of EI on a two-electron system has been performed by launching a wave packet (WP) on an excited state of $I_2{}^{2+}$ correlating with the $I^{2+} + I$ dissociation limit, through multiphoton ionization by an intense pump pulse. Then a temporally delayed probe pulse ionizes the WP to the $I_2{}^{3+}$ state which dissociates to I^{2+} and I^+, allowing the ionization rate to be measured as a function of R [10]. EI of $I_2{}^{2+}$ is found at a certain critical internuclear distance when the field is polarized along the molecular axis, and the effect disappears when the field has perpendicular polarization, just as predicted. However, in this experiment, the molecule is already in the ionic states, and so it is not clear if the mechanism is the same as that for the covalent ground state. Indeed, there are actually many different molecular configurations, even just for diatomics (see Table I), that may show EI and only a few have been fully studied experimentally, especially through pump-probe techniques.

In this work, we use a pump-probe technique and choose the excited B state of neutral I_2 as an intermediate state to study EI, as shown in Fig. 1. By launching a WP in the B state with a pump pulse [11], we obtain the R-dependent ionization rates with a temporally delayed probe pulse as the WP evolves in the B state. In addition, since the ground-state to B-state optical transition dipole moment is parallel to the internuclear axis, the molecules excited to the B state will be highly aligned along the field polarization of the pump pulse, allowing for angle-dependent measurements of ionization rates by changing the polarization of the pump pulse with respect to the probe pulse. From this work, we find a peak in the ionization rate at R_c in the parallel case, and the peak gradually goes away as the angle increases to 90°, as predicted by CREI [6]. Indeed, we find that $R_c = (3.02 \pm 0.01)/I_p$ at a wavelength of the pump pulse $\lambda_{\text{pump}} = 513$ nm and $R_c = (3.03 \pm 0.03)/I_p$ at $\lambda_{\text{pump}} = 500$ nm, in very good agreement with the theoretical prediction of $R_c = 3/I_p$ [5,12], where I_p is the ionization potential of the separated atom.

In this work, we experimentally study EI in a neutral molecule. This is significant as virtually all strong field experiments start with neutral molecules, in particular, High Harmonic Generation (HHG) [13–15] from molecules, Lochfrass [16–19], suppressed ionization [20], and coherent control [21,22]. In all of these cases, ionization of the neutral molecules is the critical first step.

II. EXPERIMENT

The experiments are performed with a home-built ultrafast Ti:sapphire laser system and a TOPAS (optical parametric

TABLE I. A summary of studies of EI, including both one-electron and two-electron systems.

Electron system	States	Properties	Mechanism
One-electron	σ states of H_2^+ [1,2,4,6,7]	EI in parallel case (both theoretical and experimental), not in perpendicular case (needs experiment)	CREI
	π or δ states of H_2^+ [7]	No EI (needs experiment)	CREI
Two-electron	σ states of H_2 [8,9]	EI in parallel case, perpendicular case unknown (needs experiment)	Ionic states as doorway states
Two-electron	Ionic excited state of I_2^{2+} [10]	EI in parallel case, not in perpendicular case (only experimental)	Similar to CREI
Two-electron	Covalent excited state of I_2, B state(σ_u state)	Similar to one-electron σ_u case (this paper)	CREI (this paper)

amplifier) system. The ionization signal of I_2^+ is recorded with a time-of-flight (TOF) spectrometer. The ultrafast laser and the TOF spectrometer are described in Refs. [23,24]. The I_2 gas is leaked effusively into the chamber with a base pressure of 6×10^{-9} torr. The Ti:sapphire laser produces pulses with a central wavelength of 800 nm, a pulse duration of 35 fs, and an output energy of up to 900 μJ at a repetition rate of 1 kHz. The output beam is split with ~90% of the energy sent into the TOPAS to generate a pump beam and the rest is used as a probe beam. The pump pulses have a central wavelength of 513 or 500 nm, a duration of 50 fs, and an energy of up to 2 μJ. The pump and probe beams are parallel but offset in space and focused by a 3-in.-focal-length silver spherical mirror inside the TOF chamber. An aperture is used to reduce the energy of pump beam to 0.5 μJ in order to decrease ionization by the pump pulse and also increase the focus spot in the chamber. This creates a more uniform focal volume for the probe pulse. The beam radius and the intensity of the pump beam at the focus are 48 μm and 1.4×10^{11} W/cm^2, respectively, while those of the probe beam are 8 μm and 1.4×10^{13} W/cm^2 (to singly ionize the I_2), respectively. The temporal delay of the two beams is adjusted by a computer-controlled translational stage and the spatial overlap is optimized by maximizing an I^{2+} signal resulting from ionization of the B state.

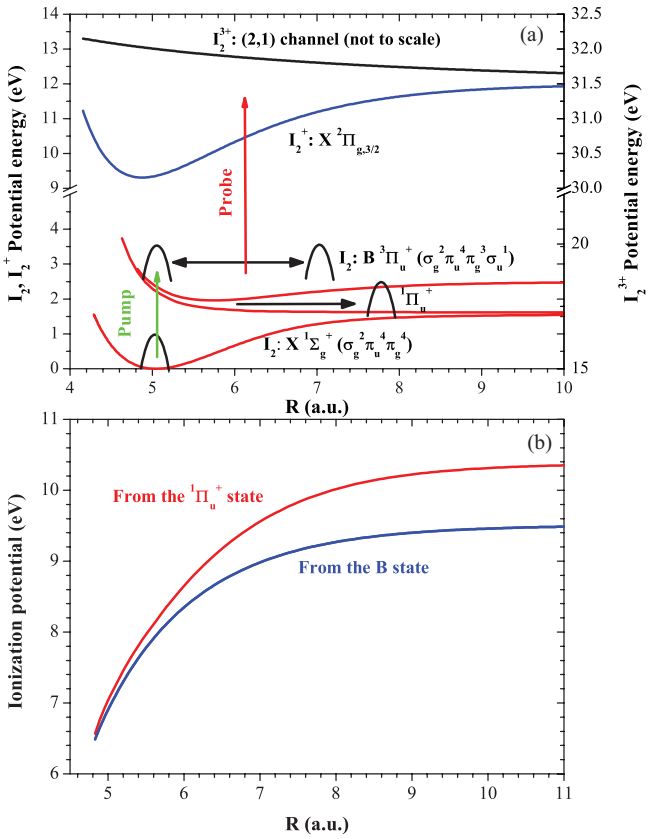

FIG. 1. (Color online) (a) Potential curves and pump-probe experimental scheme. The wavelength of the pump and probe pulses are 513 nm, and 800 nm, respectively. (b) The ionization potentials of the B state and the $^1\Pi_u^+$ as a function of R.

In the experiment, we first measure the B-state alignment as it is important for measuring the angular dependence of the ionization rate. We use a linearly polarized pump pulse to align the molecules excited to the B state, and then use a horizontally polarized probe pulse to ionize those molecules to I_2^{3+}, which dissociates into $I^{2+} + I^+$, the (2,1) channel. The polarization of the pump pulse is rotated from 0° to 180° with a $\frac{1}{2}\lambda$ plate and the I^{2+} signal is recorded by the TOF spectrometer at each angle at a fixed pump-probe delay (0.3 ps after T_0, the temporal overlap of the pump and probe pulses). Since $\frac{1}{2}\lambda$ plates are used to control the polarization angle of both beams, some residual ellipticity is introduced. However, the ellipticity was measured to be less than 1.5%. The angular dependence of the B state is shown in Fig. 2, in which the data from 180° to 360° are the inversion of the data from 0° to 180° with respect to the origin. The data are fitted by $A\cos^2(\theta - \theta_0) + B$, with $A = 0.019\,12$, $\theta = 0°$, and $B = 0$.

From Fig. 1, the pump pulse populates not only the B state, but possibly the $^1\Pi_u^+$ state which can also be ionized by the probe pulse [25]. Different from the B state, the optical transition dipole moment from the ground state to the $^1\Pi_u^+$ state is perpendicular to the molecular axis and may contribute to the signal, especially near 90°. However, the coupling from the ground state to the $^1\Pi_u^+$ state is weak at 513 nm [26], especially compared to the wavelength used in Ref. [25]. From Fig. 2, the weak, almost zero, I^{2+} signal at $\theta = 90°$ shows that the $^1\Pi_u^+$ state has little effect in this experiment.

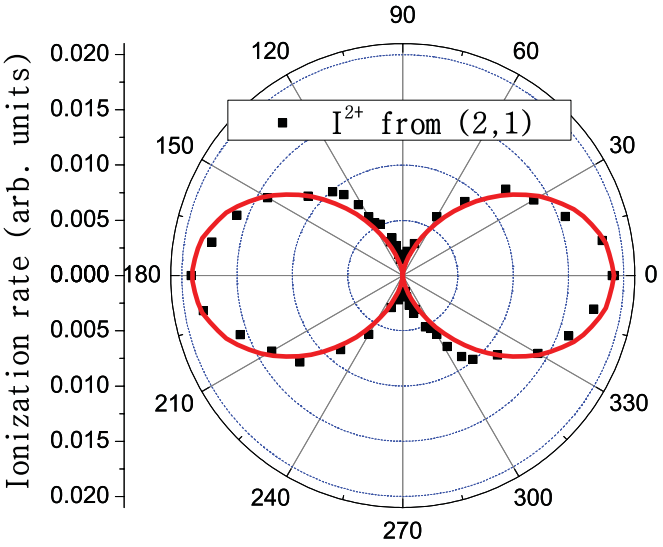

FIG. 2. (Color online) Angular dependence of the B state. The solid square data points are the experimental results, obtained by integrating I^{2+} signals in the (2,1) channel from ionization of the B state. The intensities of pump and probe beams are 1.4×10^{11} W/cm^2 and 5.6×10^{13} W/cm^2, respectively. The red curves are the fit of the data points by $A\cos^2(\theta - \theta_0) + B$, with $A = 0.01912$, $\theta = 0^\circ$, $B = 0$.

III. RESULTS

The ion signals of I_2^+ as a function of pump-probe delay $S(\tau)$ at different θ are measured with a step size of 0.030 ps, as shown in Fig. 3, for $\theta = 0^\circ$, 40°, and 90°. At each angle, the ionization peaks at a delay of around 0.33 ps.

There are two possible explanations for the peaks at ~0.33 ps in Fig. 3: (1) as the WP evolves in the B state [see Fig. 1(a)], the ionization rate increases as R increases and finally it reaches a maximum at the outer turning point;

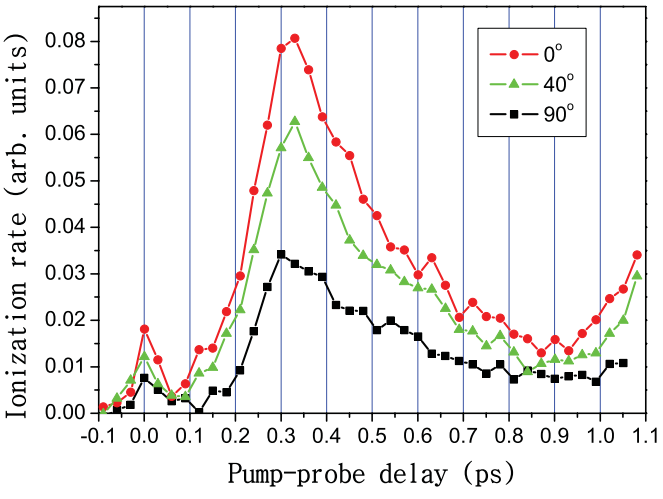

FIG. 3. (Color online) Ionization signals S of I_2^+ versus pump-probe delay τ at three different angles: $\theta = 0^\circ$, 40°, and 90°. The step size is 0.030 ps. The pump pulse has an energy of 0.5 μJ giving an estimated intensity of 1.4×10^{11} W/cm^2, and the probe pulse has an energy of 1 μJ giving an estimated intensity of 1.4×10^{13} W/cm^2. The delay of 0 ps represents T_0.

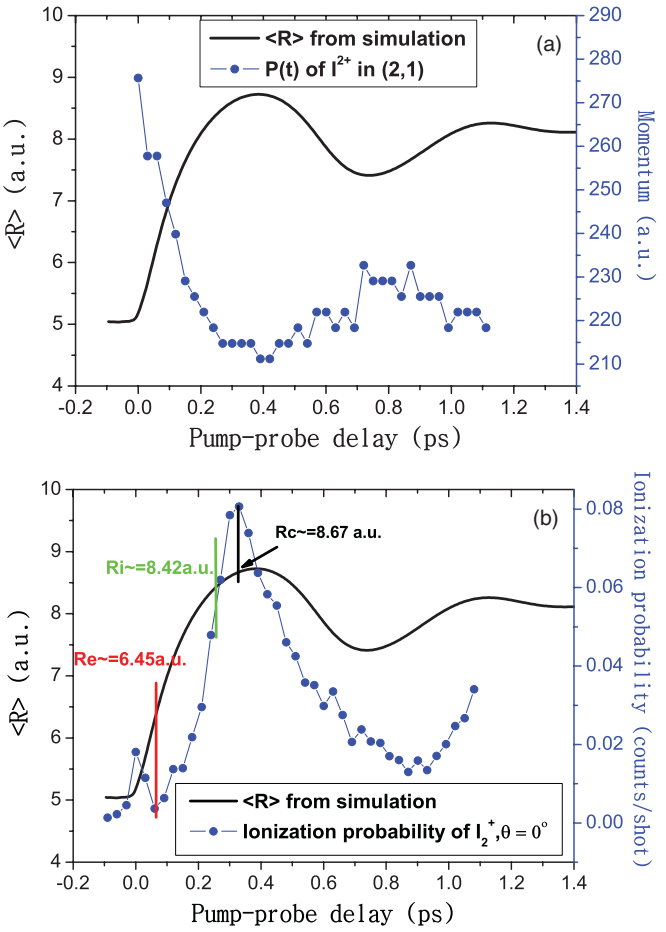

FIG. 4. (Color online) (a) The simulation of $\langle R\rangle(t)$ of the WP in the B state and the momentum $P(t)$ of I^{2+} in the (2,1) channel ionizating from the B state. (b) The simulation of $\langle R\rangle(t)$ of the WP in the B state and the ionization signal S of I_2^+ versus the pump-probe delay τ at $\theta = 0^\circ$. In the simulation, the first nine vibrational states of the X state are included as the initial state. The temperature is 300 K, the peak intensity is 1.4×10^{11} W/cm^2, $\lambda_{XB} = 513$ nm, and the pulse duration is 50 fs.

(2) there is a critical internuclear separation R_c. The rise in ionization rate as R increases cannot be attributed to simple tunneling, because the tunneling rate is a strong inverse function of the ionization potential and the ionization potential of the B state is an increasing function of R [see Fig. 1(b)], resulting in a decreasing tunneling ionization rate with R. To determine whether the peak occurs at or before the outer turning point, we obtain $\langle R\rangle(t)$ of the WP in the B state from theoretical simulations and compare it with the measurements of the momentum time evolution $P(t)$ of the WP in the (2,1) channel, as shown in Fig. 4(a). The outer turning point is reached at 0.40 ps, which is consistent with the minimum momentum from the data, while the peak is at 0.33 ps in Fig. 3. Since the peak is 0.07 ps before the outer turning point, this corresponds to a critical separation R_c. However, if the peak is due to EI at R_c, one would expect there to be another peak of the ionization rate as the WP returns, approximately at 0.47 ps, 0.07 ps after the outer turning point. None of the three curves in Fig. 3 show the expected double-peak structure. However, numerical simulation shows that the disappearance

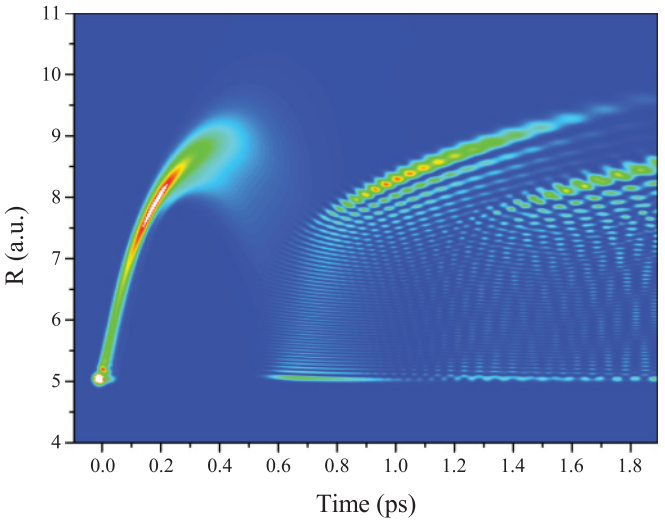

FIG. 5. (Color online) Simulation of $R(t)$ of the WP in the B state. The condition is the same as that in Fig. 4.

of the second peak is due to the dephasing and spreading of the WP. From the simulation of the WP in the B state in Fig. 5, we can see that the WP is narrow during the first half period, but starting from 0.40 ps it spreads quickly. Thus at 0.47 ps, the WP is too broad to show the ionization peak.

Nevertheless, to confirm our interpretation, we repeated the experiment with a pump pulse centered at 500 nm. This will start the WP higher up in the B-state potential and allow the WP to reach a larger R. If the ionization peak found at 513 nm was somehow related to the outer turning point, the peak with the 500-nm pump should move to longer delays. As it turns out, the peak occurs at a shorter delay, as shown in Fig. 6(a). The WP moves a bit faster with the 500-nm pump and reaches R_c sooner. We obtain the corresponding R at each pump-probe delay according to the simulation results of $\langle R\rangle(t)$ in Fig. 4(b). Plotting both data sets as a function of R [as shown in Fig. 6(b)] gives the same value (within the error bars) for R_c: $R_c = 8.67 \pm 0.03$ a.u. (513 nm) and 8.71 ± 0.09 a.u. (500 nm). In addition, we find that the ionization rate is enhanced by a factor of 22 at R_c compared to the minimum rate.

Having established that the peak in each curve in Fig. 3 is due to EI at R_c, we compare the angular dependence of the ionization rates (see Fig. 7) at three time delays, 0.33 ps (R_c), 0.26 ps (R_i, intermediate R), and 0.07 ps, corresponding to R values of 8.67, 8.42, and 6.45 a.u., respectively. The latter value is the smallest delay (i.e., closest to R_e, the equilibrium internuclear separation) that could be measured without significant temporal overlap of the pump and probe pulses. The probe pulse is horizontal, and the pump pulse is rotated from 0° to 180° with respect to the probe pulse. The data from 180° to 360° are from the inversion of the data from 0° to 180° with respect to the origin.

As seen in Fig. 7, the ionization rate at R_c at 90° is nonzero, and it corresponds to the peak at 90° in Fig. 3. Since the B state has a $\cos^2(\theta)$ distribution, even if the probe pulse is polarized perpendicularly to the pump pulse, there are still molecules in the direction in which the field of the probe pulse has a nonzero component and thus those molecules are singly ionized and detected, as well. As shown in Fig. 8(a), in the

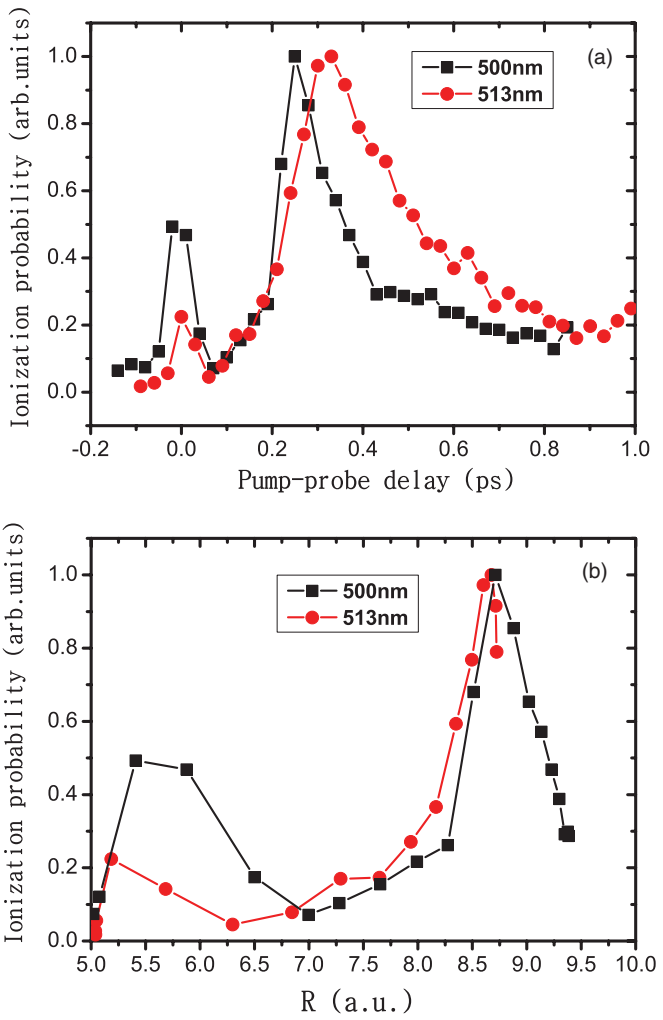

FIG. 6. (Color online) Ionization rates as a function of (a) pump-probe delay and (b) internuclear separation R at $\lambda_{\text{pump}} = 500$ and 513 nm. In panel (b), the enhancement between 5.0 and 6.5 a.u. is due to the temporal overlap of the pump and probe pulses.

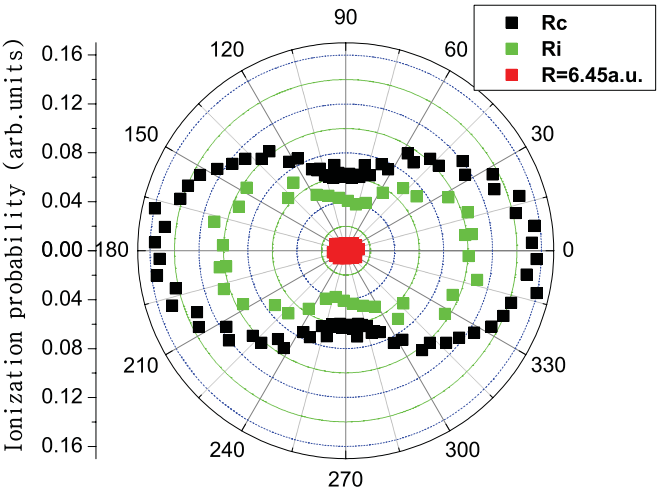

FIG. 7. (Color online) Angular dependence of ionization rates at R_c, R_i, and 6.45 a.u. The intensities of the pump and probe beams are 1.4×10^{11} W/cm^2 and 1.4×10^{13} W/cm^2, respectively, and $\lambda_{\text{pump}} = 513$ nm.

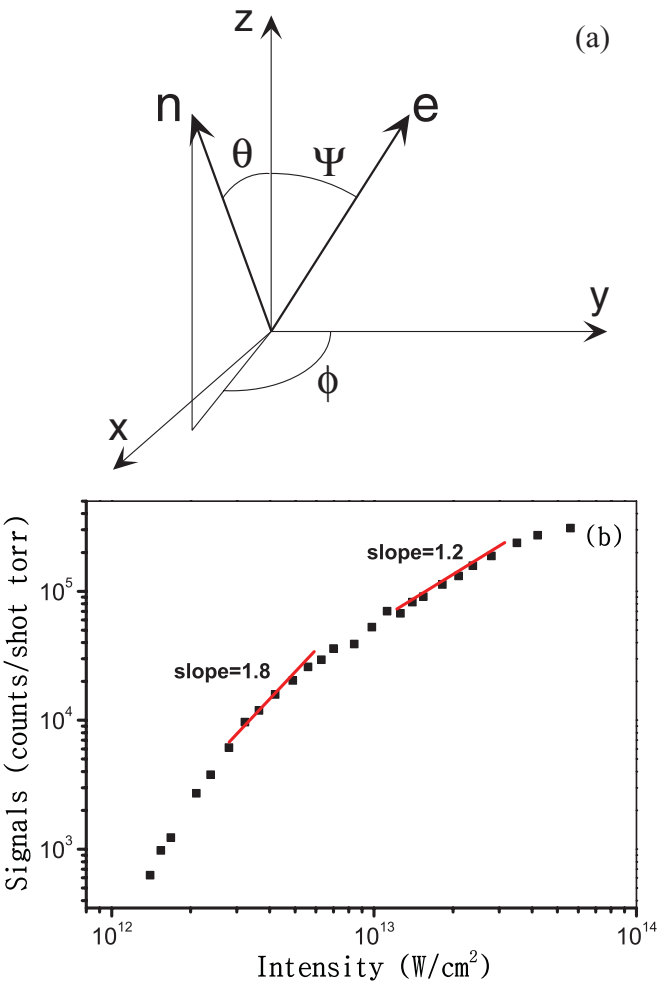

FIG. 8. (Color online) (a) The configuration of molecules in the B state and the field polarization of pump and probe pulses. (b) Measured I_2^+ ion signals as a function of the intensity of the probe pulse.

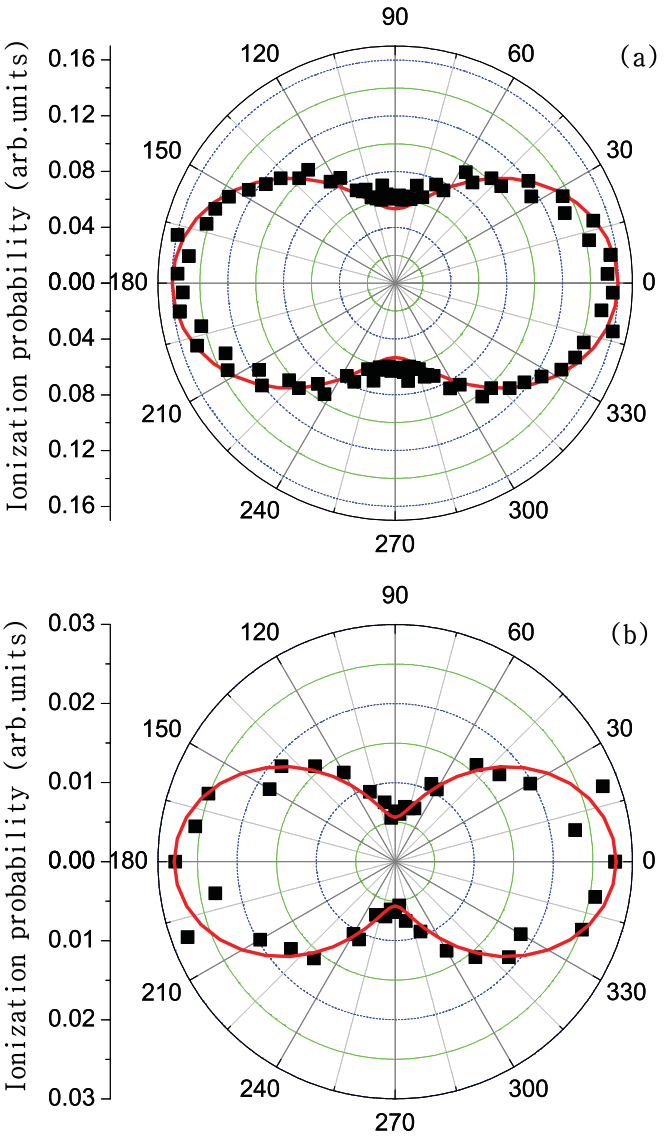

FIG. 9. (Color online) The data points are the angular dependence measurements at R_c at the intensity of (a) 1.4×10^{13} W/cm^2 and (b) 5.6×10^{12} W/cm^2, and the red smooth (thick) curves are the angular averaging calculations with (a) $n = 2$ and (b) $n = 4$.

laboratory frame, we suppose that the pump pulse is polarized in the z direction, and the probe pulse is polarized in the yz plane, in the direction $\hat{e}$, rotated by an angle Ψ from the z direction. The molecules in the direction $\hat{n}$ have a population probability of $\cos^2(\theta)$. To understand whether the peak at 90° is just an angular averaging effect of the peaks at other angles or is really EI in the perpendicular case, we calculate the angular averaging. We project the probe field in the direction $\hat{n}$, apply a multiphoton ionization model {ionization rate $\propto (E_0\hat{e}\cdot\hat{n})^n$}, and then integrate over θ and ϕ, to calculate the angular averaging effect at angle Ψ, $S(\Psi)$:

$$S(\Psi) = \int_0^{\pi}\int_0^{2\pi} (E_0\hat{e}\cdot\hat{n})^n \cos^2(\theta)\sin(\theta)d\theta d\phi,$$

where $\hat{n} = (\sin\theta\sin\phi, \sin\theta\cos\phi, \cos\theta)$ and $\hat{e} = (0, \sin\Psi, \cos\Psi)$.

While the effect of averaging does not depend strongly on n, we obtain a rough value by measuring the intensity-dependent ionization rate at R_c, as shown in Fig. 8(b). The slope of the ion-yield curve in the immediate vicinity of the intensity where the angular-dependence data were taken gives a value for n. The slopes at 1.4×10^{13} W/cm^2 and 5.6×10^{12} W/cm^2 are 1.2 and 1.8, respectively, which means $n = 2.4$ at 1.4×10^{13} W/cm^2 and 3.6 at 5.6×10^{12} W/cm^2. Then, we calculate $S(\Psi)$ at each angle Ψ between 0° and 360° for $n = 2$ and then compare with the angular dependence measurements, as shown in Fig. 9(a). From Fig. 9(a), the measurements are consistent with the angular averaging calculation. To further confirm this result, we decrease the intensity of the probe beam to 5.6×10^{12} W/cm^2 and repeat the measurements at R_c and calculations with $n = 4$, as shown in Fig. 9(b). They are still in good agreement. Therefore, we conclude that the peak at $\theta = 90°$ is just an angular averaging effect of the peaks at other angles, and itself does not show EI.

IV. DISCUSSION

EI has been rigorously studied theoretically in only a few relatively simple cases: the one-electron molecules, such as

$H_2{}^+$, and the two-electron molecule H_2. However, further work suggests the predictions from the above studies are much more general. Nevertheless, ionization from the B state of I_2 would appear to be much more complex, having features of both the one-electron and two-electron models. The B state could be considered to be a one-electron system, as the lone electron in the σ_u orbital would be the most active electron. However, neutral I_2 has ionic states ($I^+ + I^-$) which play a critical role in even-charged molecules [8,9]. In either case, the electronic structure of the excited states of I_2 is far more complex than anything previously considered.

The most basic consideration for EI in a one-electron molecule is electron localization, as, without this, EI is not possible. The condition for electron localization can be estimated from a simple model [5,12]. We start with a double-well Coulomb potential:

$$V(z,R) = -\frac{Q}{|z+R/2|} - \frac{Q}{|z-R/2|},$$

where Q is the charge on each well and z is the distance along the internuclear axis. The ionization potential of the separated atoms or ions can be approximated as QI_p for an ion of charge $(Q-1)$, where I_p is the ionization potential of the neutral molecule, and the lowering of the state as Q/R. Then electron localization occurs when the inner barrier just equals the energy of the state:

$$-\frac{2Q}{R_c/2} = -QI_p - \frac{Q}{R_c} \Longrightarrow R_c = \frac{3}{I_p}.$$

In this work, I_p for the B state of I_2 is 9.5 eV (0.35 a.u.), and $R_c = 8.67 \pm 0.03$ a.u. (513 nm) and 8.71 ± 0.09 a.u. (500 nm), which gives $I_p R_c = 3.03 \pm 0.01$ (513 nm) and 3.05 ± 0.03 (500 nm), respectively, remarkably close to the prediction of 3. From this, we must conclude that electron localization is the overriding requirement for EI at R_c and that the conditions for localization can be deduced from very simple considerations, despite the specific complexities of particular molecules. Interestingly, the simple model of Refs. [5,12] was extended in Ref. [27] to include field-induced changes in the energy levels. This gives the result $R_c = 4/I_p$, which is definitely inconsistent with our results. Clearly, more experimental and theoretical work is required to fully understand the phenomenon of R_c.

V. CONCLUSION

For the first time, we obtain fully R and θ resolved measurements of R_c in a homonuclear neutral diatomic molecule. The angular distribution of the B state of I_2 is obtained, and it shows the expected $\cos^2(\theta)$ distribution. When the laser field is parallel to the molecular axis, the B state shows EI at a certain critical separation R_c with an enhancement factor of 22, and as the angle between the two increases, the ionization peak at R_c decreases and finally disappears in the perpendicular case. The EI of the B state of I_2 can be explained by CREI, and the determination of R_c shows that R_c can be precisely predicted by a simple model of electron localization. EI is a very general phenomenon which has yet to be fully explored.

ACKNOWLEDGMENT

We would like to acknowledge support from the NSF under Grant No. PHYS-0968799.

[1] G. N. Gibson, M. Li, C. Guo, and J. Neira, Phys. Rev. Lett. **79**, 2022 (1997).
[2] Th. Ergler, A. Rudenko, B. Feuerstein, K. Zrost, C. D. Schroter, R. Moshammer, and J. Ullrich, Phys. Rev. Lett. **95**, 093001 (2005).
[3] E. Constant, H. Stapelfeldt, and P. B. Corkum, Phys. Rev. Lett. **76**, 4140 (1996).
[4] T. Zuo and A. D. Bandrauk, Phys. Rev. A **52**, R2511 (1995).
[5] T. Seideman, M. Yu. Ivanov, and P. B. Corkum, Phys. Rev. Lett. **75**, 2819 (1995).
[6] T. K. Kjeldsen, L. B. Madsen, and J. P. Hansen, Phys. Rev. A **74**, 035402 (2006).
[7] G. Lagmago Kamta and A. D. Bandrauk, Phys. Rev. A **75**, 041401(R) (2007).
[8] I. Kawata, H. Kono, Y. Fujimura, and A. D. Bandrauk, Phys. Rev. A **62**, 031401(R) (2000).
[9] E. Dehghanian, A. D. Bandrauk, and G. L. Kamta, Phys. Rev. A **81**, 061403(R) (2010).
[10] E. Constant, H. Stapelfeldt, and P. B. Corkum, Phys. Rev. Lett. **76**, 4140 (1996).
[11] L. Fang and G. N. Gibson, Phys. Rev. A **81**, 033410 (2010).
[12] J. H. Posthumus, L. J. Frasinski, A. J. Giles, and K. Codling, J. Phys. B **28**, L349 (1995).
[13] See, e.g., E. V. van der Zwan, C. C. Chirila, and M. Lein, Phys. Rev. A **78**, 033410 (2008), and references therein.
[14] J. Itatani *et al.*, Nature (London) **432**, 867 (2004).
[15] E. Hijano, C. Serrat, G. N. Gibson, and J. Biegert, Phys. Rev. A **81**, 041401(R) (2010).
[16] T. Ergler, B. Feuerstein, A. Rudenko, K. Zrost, C. D. Schroter, R. Moshammer, and J. Ullrich, Phys. Rev. Lett. **97**, 103004 (2006).
[17] E. Goll, G. Wunner, and A. Saenz, Phys. Rev. Lett. **97**, 103003 (2006).
[18] L. Fang and G. N. Gibson, Phys. Rev. A **78**, 051402(R) (2008).
[19] L. Fang and G. N. Gibson, Phys. Rev. Lett. **100**, 103003 (2008).
[20] J. Muth-Bühm, A. Becker, and F. H. M. Faisal, Phys. Rev. Lett. **85**, 2280 (2000).
[21] C. Trallero-Herrero, D. Cardoza, T. C. Weinacht, and J. L. Cohen, Phys. Rev. A **71**, 013423 (2005).
[22] C. Trallero-Herrero and T. C. Weinacht, Phys. Rev. A **75**, 063401 (2007).
[23] L. Fang and G. N. Gibson, Phys. Rev. A **75**, 063410 (2007).
[24] G. N. Gibson, R. N. Coffee, and L. Fang, Phys. Rev. A **73**, 023418 (2006).
[25] J. J. Larsen, I. Wendt-Larsen, and H. Stapelfeldt, Phys. Rev. Lett. **83**, 1123 (1999).
[26] Joel Tellinghuisen, J. Chem. Phys. **58**, 2821 (1973).
[27] S. Chelkowski and A. D. Bandrauk, J. Phys. B **28**, L723 (1995).